Mechanical properties of Dungeness crab based chitin

AUTHORS: Michael Ikpi Ofem (PhD), Musa Muhammed (M.Eng) and Muneer Umar (PhD)

ABSTRACT: Chitin from Dungeness crab was extracted by chemical processes. Chitin film prepared by a modified method was characterised for mechanical, thermal and structure related properties. Depending on the gauge length the stress at failure decreased from 63.9MPa at 5mm gauge length to 36.6MPa at 50mm gauge length. TGA based thermal characterisation shows a two stage weight losses, one due to water and the other related to saccharide rings degradation. In the DSC no glass transition was observed whereas the Raman spectrum indicated an α -chitin polymorph with the amide band splitting into two peaks at 1653 and 1621cm.-1 XRD spectrum showed four peaks at $2\theta = 9.48^{\circ}$, 21.05° , 22.98° and 25.96° with a crystalline index of 86%. SEM images showed rough surfaces with fibril like morphology without any trace of porosity.

KEY WORDS: Dungeness crab shell, Chitin, Gauge length, Mechanical properties.

1.0 INTRODUCTION

Bio composites have become attractive because of their wide applications and low cost. The interest in bio composites is growing due to the high performance in mechanical properties. Research into biomaterials is to get composite materials with comparable or even better properties (compared to conventional engineering materials) as well as a means for convenient disposal made available due to biodegradability. Undoubtedly, the mechanical properties of any composite material help in determining its applications window among other things. A lot of biological materials have attained better mechanical properties compared to conventional materials [1]. This could be attributed to the highly hierarchically organised structural level common to biomaterials. A lot has been reported on the microstructure of bio-composites. For instance, Melnick et al., [2] in their paper, "Hardness and Toughness of exoskeleton materials in the stone crab, Meippe mercenaria" confirmed that the dark pigment in the stone crab indicates a form of structural change. These changes were noticed in the level of porosity between the black and the yellow coloured exoskeleton materials of the same crab. The level of porosity was found to decrease as the colour changes from black to yellow. In their study regarding the relationship between structure and mechanical properties of the sheep crab(loxorhynchus grandis), Chen et al., [3] and Fabritius et al., [4] found a highly mineralized chitin-protein fibres arranged in a twisted Bouligand pattern in x-y plane with a high density of pore canal tubules in the direction normal to the surface(z-direction). Periwinkles (Turritella communis) are small edible species of medium-sized sea snails of the marine gastropod molluscs. Some research into

the properties of periwinkles shells are geared towards its possible usage as a replacement for concretes as reported by Adewuyi and Adegoke [5] and Osarenmwinda and Awaro [6]. Huang and Xiao [7] focused on the mechanical properties of quaternized polysulfone/benzoyl periwinkle shells blends.

Chitin is one of the most abundant biopolymers and the most widely spread amino-polysaccharide found in seashells. It is found in the exoskeleton of crustaceans and insects. It can also be found in the cell walls and structural membranes of fungi, yeast and green algae. The exoskeletons compose of lipids, pigments, proteins and trace elements. Due to the wide application of chitosan(alkaline hydrolysis of chitin); different methods of chitin extraction have been published. Chitin can be extracted by fermentation and enzymatic methods. While the extraction of chitin by fermentation is very expensive, enzymatic extraction does not denature the chitin. Another method that has been widely reported is the chemical method [8], [9], [10], [11], [12] which make use of plenty alkaline, this is the method that is been reported here. This work therefore, intends to investigate the mechanical performance of chitin extracted from dungeness crab (Cancer magister) shells at different gauge lengths, study the structure and morphology of the chitin film using Raman Spectroscopy, X-Ray diffraction, thermo gravimetric analysis, Differential Scanning Calorimetric and Scanning Electron Microscopy.

- 2.0 Experimental Methodology
- 2.1 Extraction of Chitin

Dungeness crab (Cancer magister) was purchased from Chinese restaurant Faulkner Street Manchester England, NaOH, HCl, NaClO₂, and KOH were purchased from Sigma Aldrich UK. Extraction and purification of chitin from dungeness crab shells were done according to the procedure reported in the literature method [8],[9],[10], [11],[12]. Coarsely crab shells were cleaned with water by stirring the broken shells in a big beaker, the shells were filtered and the process was repeated until all impurities were removed. The cleaned crab shells were dried in an oven at temperature of between 70 and 80°C for 6 hours and then grinded to obtain finer particles. 30g of grinded dried shells were added to 40% NaOH (1:10w/v) solution. The mixture was boiled under stirring at a temperature of 60-70°C for about one hour. The shells were then filtered and the process was repeated four times to ensure that the filtrate is clear and colourless. The shells were washed with demineralised water till a neutral pH was attained. HCl was slowly added to the shell (1:15w/v) and the mixture stirred at room temperature for about 25 minutes without observing the escape of gaseous substances. The product was filtered, washed with demineralised water and then dried in an oven at a temperature of 70°C for 12 hours. Residual protein was removed by stirring the chitin at room temperature in 5wt% KOH solution for six hours. The Chitin was bleached in a mixture of NaClO2 and Sodium acetate buffer solutions for six hours at temperatures of between 70 and 80°C under stirring. At every two hours interval, the solution is rinsed by centrifugation at 8000rpm for 20 minutes. Dilute HCl was added to the purified chitin to raise the pH to 3 and then ultrasonification was applied for 2 minutes, filtered and then tried in an oven for 10 hours at a temperature of between 70 and 80°C.

2.2 Preparation of Chitin Films

Chitin films were made according to a modified published [13,14]. Purified chitin was roughly crushed in a domestic blender, and then vacuum sieved using a Buchner filter funnel having an approximate size of 1.4 mm. The sieved chitin was dispersed in water to make 0.5 wt % content. The pH value was adjusted to 3 by adding few drops of acetic acid. The solution was stirred magnetically over night at room temperature. The suspension was vacuum filtered using Whitman filter paper. The chitin nanofibre was pressed for up to 60 minutes at a temperature maintained at

80-90°C. The film was dried in an oven at a temperature of 50 °C for 48 hours.

2.3. Characterisations of film

Mechanical properties of samples were tested, in tension using a Universal Testing Machine - UTM (Instron 5567). Ten samples were tested at a strain rate of 3mm/min for each gauge length. All specimens were conditioned at a temperature of 23±2 °C and 50±5 % relative humidity for 48 hours before testing. A ReniShaw system 1000 spectrometer was used to collect Raman spectra from the sample using a 785 nm near infrared laser. A ×50 working distance lens was used to focus the laser on the surface of the samples to a spot size of ~1-2µm. A mixed Lorentzian/Gaussian function was used to determine the peak positions for Raman bands. Crystalline determinations of the fibres were performed using PhilipsTM X"Pert powder diffractometer with a 1.79 Å Cobalt X-ray sources. The samples were scanned from 2θ = 5-50° θ in step sizes of 0.05° at 6 seconds per step. The crystalline Index (CI) was calculated from the normalised diffractograms using Focher et al., [18] and Cárdenas et al., [19] methods. Equation 1 is the crystalline index equation where I_{110} is the intensity of the diffraction (110) at $2\theta \approx$ 19.5° representing the crystalline packing of the chitin structure, and Iam is the minimum intensity at the amorphous region between the I₁₁₀ and I₀₂₀ peaks. Equation 2, the Bragg equation [24] was used to calculate the dspacing where θ is the Bragg diffraction angle, λ the wave length.

$$Cr_{110} = \frac{I_{110} - I_{am}}{I_{110}} X 100$$

$$d = \frac{\lambda}{2\sin\theta}$$

A TA Q100 heat-flux differential scanning calorimeter was used to investigate the thermal properties of the film. Samples were heated from room temperature to 250° C at 10 ° C min-1 under 50min-1 nitrogen purge gas flow. A NETZSCH Simultaneous Thermo gravimetric Analysis (STA) 449C instrument was used to study the degradation temperature and weight loss pattern as a function of temperature. The morphologies of the samples were investigated using a FEM-SEM XL30 scanning electron microscope. Samples were first carbon coated to enhance

electron flow and imaged using a spot size of 3, with × 50 magnifications and an acceleration voltage of 8 kV.

3.0 Results and Discussion

Figure 1 show the stress-strain curves for chitin film for different gauge lengths, while Figures 2-4 shows the Young modulus as a function of inverse gauge length, stress and strain at failure as a function of gauge length respectively. The trend shows that the higher the length of the tested materials the lower the stress at failure, the percentage decrease gradually increases from 6.1 at 10mm gauge length to 15.2 at 50 mm gauge length. This decrease is thought to be due to defects, the larger the specimen size; the more probable it is to have defects. This result is in agreement with Griffith's theory [15], where a thinner material tends to be close to its theoretical strength. In other words the gradual decrease in tensile strength is an indication of the presence of strength limiting defects, [16] this defects could be voids, minor cuts, non-uniform thickness of films etc.

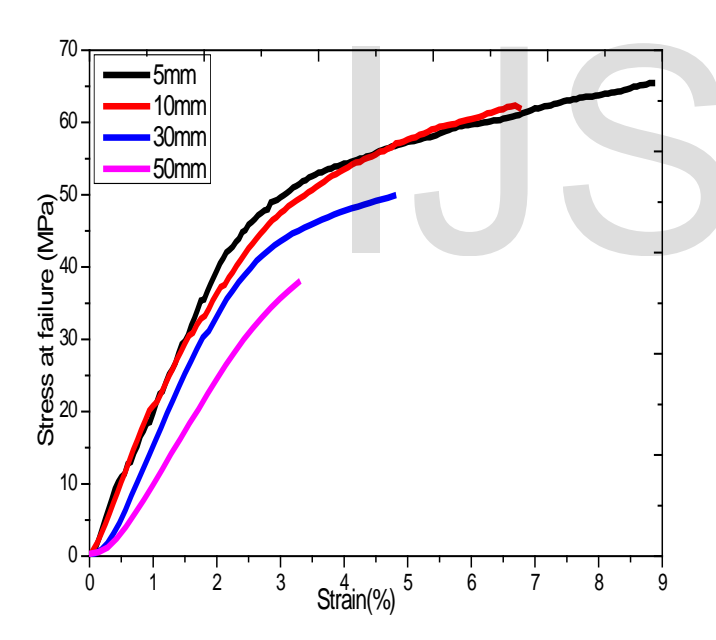


Figure 1: Stress-strain curves for chitin film sheets at different gauge lengths

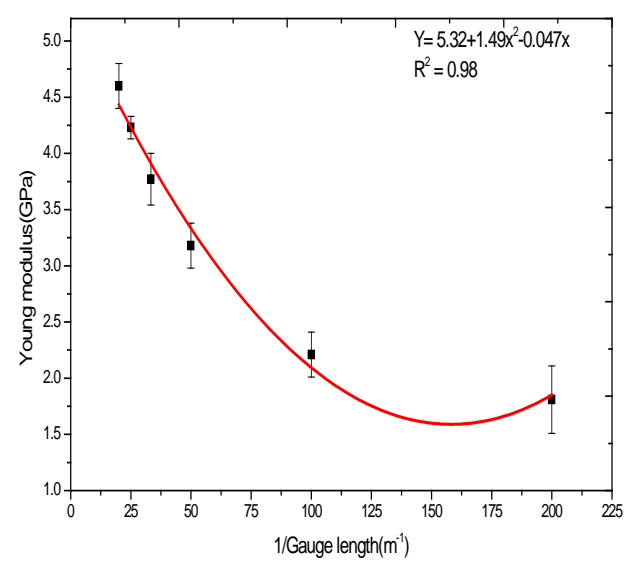


Figure 2: Young modulus as a function of gauge lengths for chitin film

There was an increase in strain as the gauge length decreases. The decrease in strain gradually increases from 14.5% at 10mm gauge length to a maximum of 21.7 % at 30mm and finally drops to 10.7% at 50mm gauge length. Higher ultimate elongation values are associated with increased toughness. It is also observed that the higher the gauge length the smaller the modulus. This may be attributed to strength limiting defects. The mechanical properties obtained here are comparable with various reported properties in the literature. Depending on the method of chitin film preparation, Yusof et al., [17] reported Young's modulus between 1.2 and 3.7 GPa while the tensile strength ranged between 38.3 and 77.2 MPa and the % strain between 4.7 and 21.3 %. Ifuku et al., [14] however reported a Young's modulus of 2.5 GPa and a tensile strength of 40 MPa for chitin film.

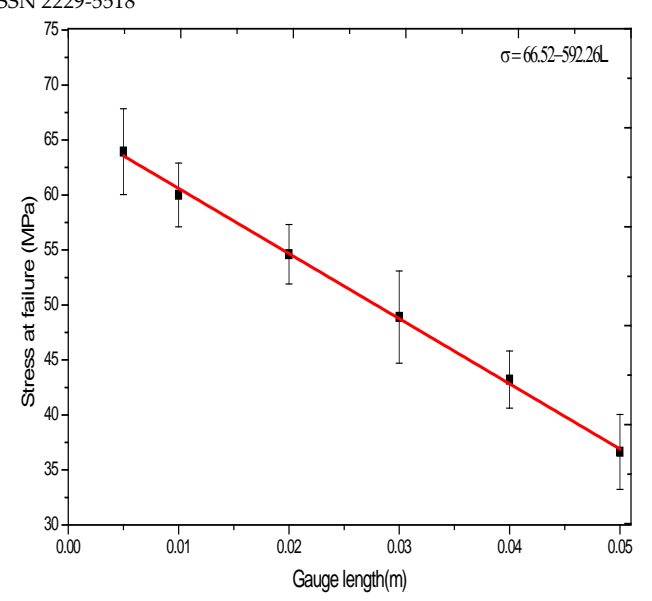


Figure 3: Stress at failure as a function of gauge lengths for chitin film

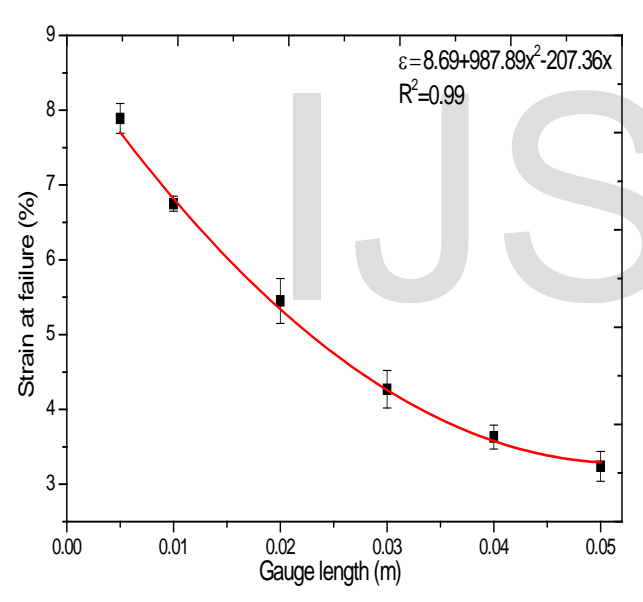


Figure 4: Strain as a function of gauge lengths for chitin film

Figure 5 is a Raman spectrum obtained from chitin film. The assigned Raman band peaks are based on literature [18], [19], [20]. Strong peaks were observed at 1653 and 1621 cm⁻¹ [amide band], 1416, 1376, 1327 cm⁻¹ [CH₂ deformation, -CH₃ symmetrical deformation mode and CH₂ wagging respectively], 1263 and 1205 cm⁻¹ [NH bending vibration and amide III respectively], 1109, 709 ,650 cm⁻¹ [C-O-C vibration of chitin-ether OH out- of-plane band and NH(amide) respectively], 1059, 954, 896 cm⁻¹ [C-O

stretching, C-O ring vibration and ring respectively]. The chitin spectra here are typical of α -chitin [18], [19], [20].

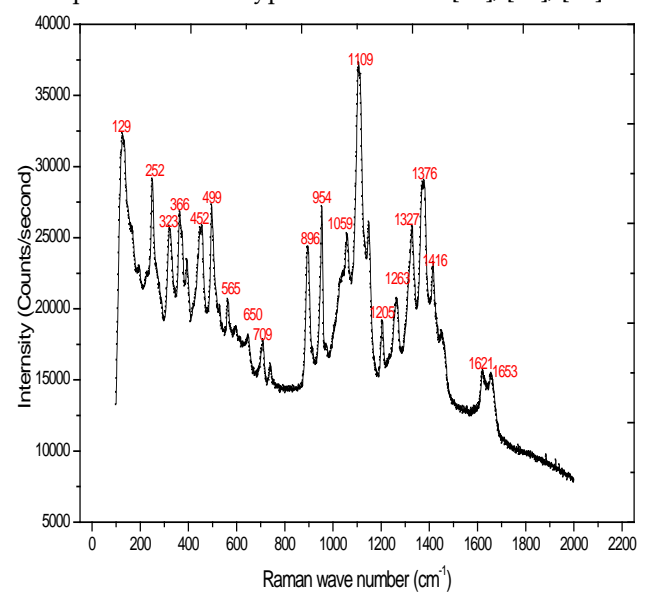


Figure 5: Raman spectrum obtained from a chitin nanofibre sheet

Figure 6 shows an X-ray diffractogram of a chitin nanofibre film. From the figure two strong and two weak peaks are observable. These are located at $2\theta = 9.48^{\circ}$, $2\theta = 21.05^{\circ}$ (strong), $2\theta = 22.98^{\circ}$ and $2\theta = 25.96^{\circ}$ (weak) corresponding to d-spacings of 9.66 Å, 4.46 Å, 8.61 Å and 3.88 Å respectively. The corresponding Miller indices are,(100), (130), (101) and (013) respectively. Cardena et al., [19], Jang et al.,[21] and Kim et al., [22] reported crystalline peaks at around 2θ= 9.22-9.6°, 19.5-19.6°, 21.1° and 23.7-26.3°, depending on the source of the α -chitin, while β -chitin exhibits peaks at 2θ = 9.1° and 20.3° an indication of lower crystallinity of β -chitin. Generally a typical α -chitin diffraction pattern shows strong reflections at $2\theta = 9-10^{\circ}$ and $2\theta = 20-21^{\circ}$ while minor reflections occurs at higher $2\theta =$ 26.4° and higher values of 2θ [23]. The result obtained here is an indication of higher crystallinity when compared to theirs, to confirm this, 86 % crystalline index was recorded compared to between 66.3 to 81.9% reported by Cardena et al.,[19].

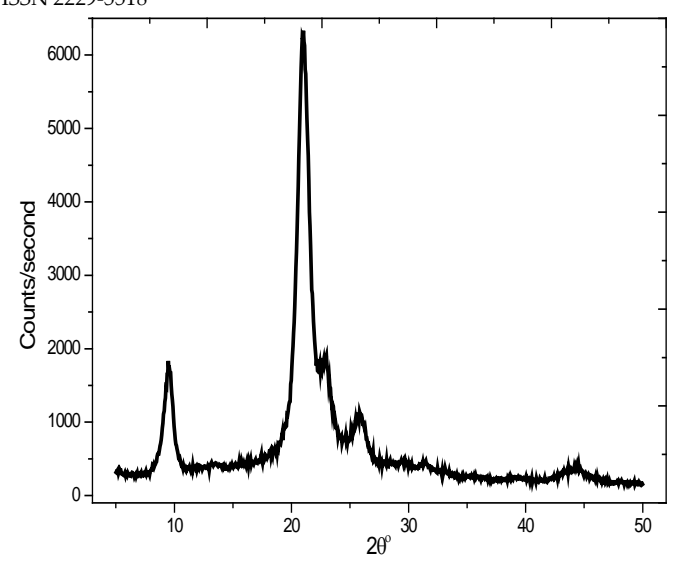


Figure 6: X-Ray Diffraction pattern for a chitin nanofibre sheet

To investigate the thermal properties using DSC, only the first heating of chitin film was recorded. Figure 7 shows the DSC heating curves of chitin. Chitin did not show any glass transition confirming earlier reports [25], [26]. A weak endothermic peak at 125°C attributed to the evaporation of chemically bounded water in the chitin [21] was also observed. Figure 8 shows the TGA curve of chitin film. Chitin shows two stages of weight loss; the 1st occurs between 50-125°C with a weight loss of ~5.3%, this is due to loss of unbound water. The second stage of degradation occurred between 250-398°C with a weight loss of 30 wt % and is ascribed to the degradation of saccharide rings [25].

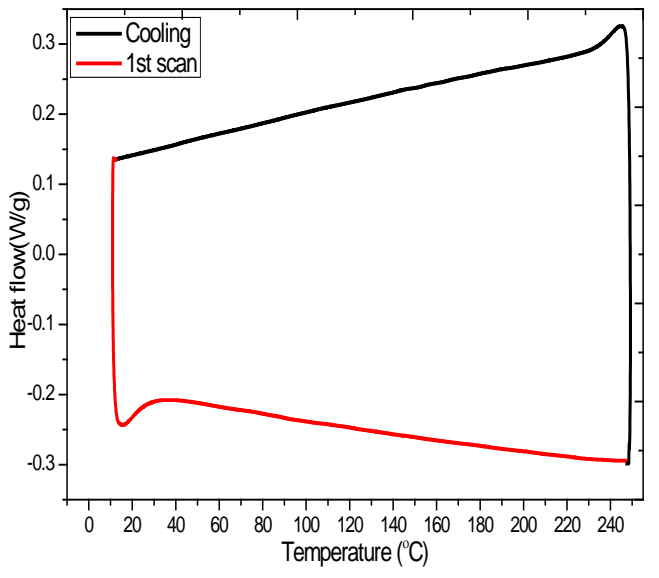


Figure 7: DSC heating curves of chitin film

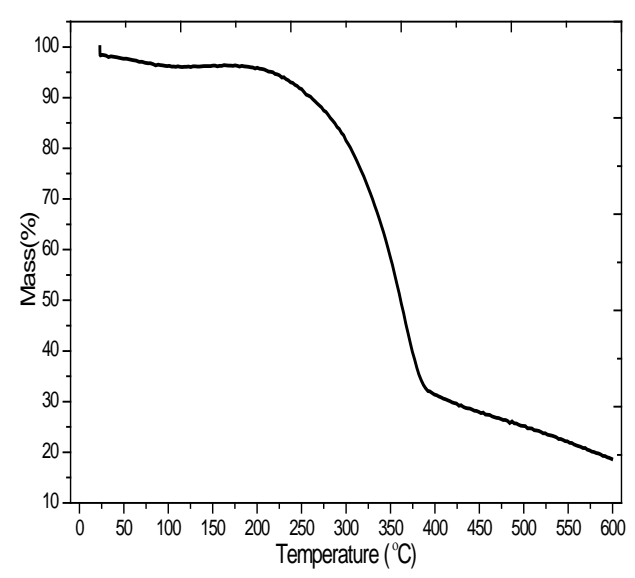


Figure 8: TGA curve of chitin film

The morphology of the chitin nanofibre sheets was studied using a scanning electron microscope (SEM) and is presented in figure 9. The figure is characterised by rough surfaces and fibril morphology. Careful observation reveals absence of porosity in all the micrographs images which is an indication of high level of molecular packing resulting into high crystalline index as earlier reported in XRD characterizations. The free surface was estimated to have thickness ranging between 39 and $68 \, \mu m$.

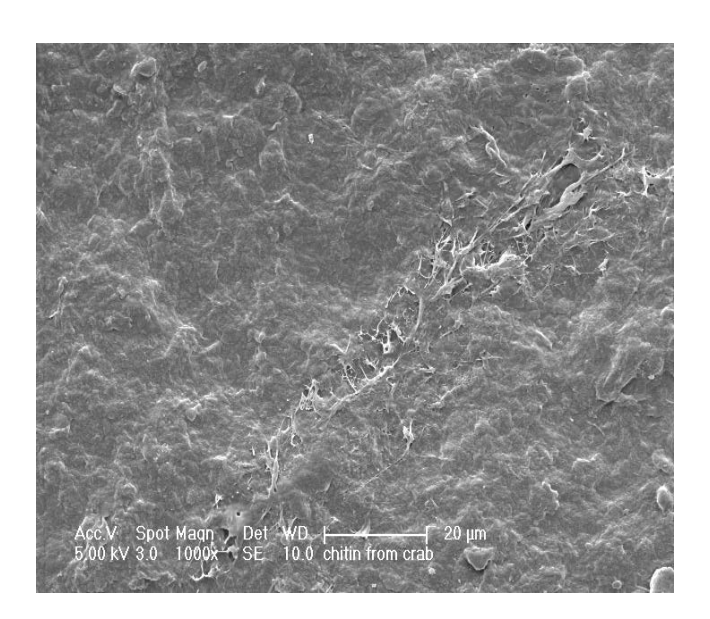




Figure 9:s Scanning electron microscope (SEM) image of a chitin nanofibre sheet

4.0 Conclusion

The performance of materials depends, among other things, on their thermal properties. Thermogravimetric analysis (TGA) and differential scanning calorimetry (DSC) are some of the techniques used to characterise the thermal properties of the materials in this study. The use of DSC determines the glass transition temperature while TGA gives an insight into the degradation behaviour. The Tg of chitin extracted from crab by chemical method could not be observed confirming earlier reported reports. Different gauge lengths give different mechanical properties that are stress and strain at failure and the Young modulus. The variation in mechanical properties was attributed to strength limiting defect some of which are non uniform thickness of film, void and minor cut on the film. While the strain and stress at failure decreases as the gauge length decreases the Young Modulus increases as the gauge length decreases. XRD characterisation shows that chitin film was highly crystalline with crystalline index of 86%. Crystalline peaks were observed at $2\theta = 9.48^{\circ}$ and $2\theta = 21.05^{\circ}$

References

- [1]. Vincent JFV. Arthropod cuticle: A natural composite shell system. Composites *Part A* 2002: 33; 1311.
- [2]. Melnick CA, Chen Z and Mechholsky Jr JJ. Hardness and Toughness of exoskeleton materials in the stone crab. Journal of Material Research 1996; 11: 2903-2907.

- [3]. Chen PY, Lin AYM, Meyers MA and McKittrick J. Structure and Mechanical Properties of crab exoskeleton. Acta Biomaterialia 2008; 4: 587-596.
- [4]. Fabritius H, Sachs C and Raabe D. Hardness and elastic properties of dehydrated cuticle from *Homarus americanus* obtained by nano indentation. Journal of Material Research 2006; 21: 1987-1995.
- [5]. Adewuyi AP and Adegoke T. Exploratory Study of Periwinkle Shells as Coarse Aggregate in Concrete Works. Journal Science Resources 2008; 4:1678-1681.
- [6]. Osarenmwinda JO and Awaro AO. The potential use of periwinkle shell as coarse aggregate for concrete. Advanced Materials Research 2009; 62:39-43.
- [7]. Huang Y and Xiao C. Miscibility and mechanical properties of quaternized polysulfone/benzoyl periwinkle shells blends. Polymer 2007; 48:371-381.
- [8]. Bader HJ and Birkholz E. Chitin from crab' Chitin Hand Book, R. A.A. Muzzarelli and M.G. Peters, Eds., European Chitin Society 1997
- [9]. Morin A and Dufresne A. Nanocomposites of Chitin Whiskers from Riftia Tubes and Poly (caprolactone). Macromolecules 2002; 35:2190-2199.
- [10]. Aranaz, I. Mengíbar, M. Harris, R. Paños, I. Miralles, B. Acosta, N. Galed, G. and Heras, Á. Functional characteristics of Chitin and Chiosan. Current Chemical Biology 2009; 3: 203-230.
- [11]. Watthanaphanit A, Supaphol P; Tamura H, Takura S and Rujiravanit R. Fabrication, structure and properties of Chitin Whiskers-Reinforced Alginate Nanocomposite Fibers. Journal of Applied Polymer Science 2008; 110:890-899.
- [12]. Al Sagheer FA, Al-Sughayer, MS and Elsabe MZ. Extraction and characterisation of chitin and chitosan from marine sources in Arabia Gulf. Carbohydrate Polymers 2009; 77:410-419.
- [13]. Ifuku S, Nogi M, Yoshioka M, Morimoto M, Yano H and Saimoto H. Fibrillation of dried chitin into10-20 nm nanofibers by a simple grinding method under acidic conditions. Carbohydrate Polymers 2010; 81:134-139.
- [14]. Ifuku S, Morooka S, Nakagaito A, Morimoto M and Saimoto H. Preparation and characterization of optically transparent chitin nanofibers/(meth)acrylic resin composites. Green Chemistry 2011; 13:1708-1711.

- [15]. Gordon JE "The science of strong materials or why you don't fall through the floor" Walker and Co., New York, 1976.
- [16]. Zhu D, Mobasher B, Erni J, Bansal S, Rajan SD. Strain rate and gage length effects on tensile behaviour of Kevlar 49 single yarn. Composites: Part A 2012; 43:2021–2029.
- [17]. Yusof NL, Lim LY and Khor E. Flexible chitin films: structural studies. Carbohydrate Research 2004; 339:2701-2711.
- [18]. Focher B, Naggi A, Torri G, Cosani A and Terbojevich M. Structural differences between chitin polymorphs and their precipitates from solutions—evidence from CP-MAS 13C-NMR, FT-IR and FT-Raman spectroscopy. Carbohydrate Polymers 1992; 17:97-102.
- [19]. Cárdenas G, Cabrera G, Taboada E and Miranda SP. Chitin characterization by SEM, FTIR, XRD, and ¹³Ccross polarization/mass angle spinning NMR. Journal of applied Polymer Science 2004; 93:1876-1885.
- [20]. Zia KM, Bhatti IA, Barikani M, Zuber M, and Bhatti HN. XRD studies of polyurethane elastomers based on chitin/1, 4-butane diol blends. Carbohydrate Polymers 2009; 76:183-187.

- [21]. Jang M, Kong B, Jeong Y, Lee C H and Nah J. Physicochemical Characterization of α Chitin, β -Chitin, and γ -Chitin Separated from Natural Resources. Journal of Polymer Science: Part A: Polymer Chemistry, 2004; 42:3423-3432.
- [22]. Kim SS, Kim SH and Lee YM. Preparation, Characterization, and Properties of β Chitin and N-acetylated β -Chitin. Journal of Polymer Science: Part B: Polymer Physics, 1996; 34:2367-2374
- [23]. Abdou, ES, Nagy, KSA, Elsabee, MZ. Extraction and characterization of chitin and chitosan from local sources. Bioresources. Technology 2008; 99:1359-1367.
- [24]. Bragg W, H and Bragg W,L. The Reflection of X-rays by Crystals. Proceedings of the Royal Society London 1913; A88(605):428-438
- [25]. Kim SS, Kim SH, Moon YD and Lee MY. Thermal characteristics of chitin and hydroxypropyl chitin. Polymer 1994; 35:3212-3216
- [26]. Kurita K, Inoue M and Harata M. Graft Copolymerization of Methyl Methacrylate onto Mercaptochitin and Some Properties of the Resulting Hybrid Materials. Biomacromolecules 2002; 3:147-152.